Available online at www.sciencedirect.com
SCIENCE DIRECT®
Analytical Biochemistry 336 (2005) 243–252
ANALYTICAL BIOCHEMISTRY
www.elsevier.com/locate/yabio

Valence and anion binding of bovine ribonuclease A between pH 6 and 8

Thomas P. Moody[a,*], Jonathan S. Kingsbury[a], Jennifer A. Durant[a], Timothy J. Wilson[b], Susan F. Chase[a], Thomas M. Laue[a]

[a] *Center to Advance Molecular Interaction Science, Rudman Hall, 46 College Road, University of New Hampshire, Durham, NH 03824, USA*
[b] *Cancer Research UK, Nucleic Acid Structure Research Group, Department of Biochemistry, The University of Dundee, Dundee DD1 5EH, UK*

Received 14 July 2004
Available online 23 November 2004

Abstract

Several studies have shown that divalent anion binding to ribonuclease A (RNase A) contributes to RNase A folding and stability. However, there are conflicting reports about whether chloride binds to or stabilizes RNase A. Two broad-zone experimental approaches, membrane-confined electrophoresis and analytical ultracentrifugation, were used to examine the electrostatic and electrohydrodynamic characteristics of aqueous solutions of bovine RNase A in the presence of 100 mM KCl and 10 mM Bis–Tris propane over a pH range of 6.00–8.00. The results of data analysis using a Debye–Hückel–Henry model, compared with expectations based on pK_A values, are consistent with the binding of two chlorides by RNase A. The decreased protein valence resulting from anion binding contributes 2–3 kJ/mol to protein stabilization. This work demonstrates the utility of first-principle valence determinations to detect protein solution properties that might otherwise remain undetected.

Keywords: Membrane-confined electrophoresis; Steady state electrophoresis; Valence; Charge of macro-ions in solution; Debye–Hückel–Henry

Though evidence of monovalent anion binding by ribonuclease A (RNase A) has been contradictory [1,2], the importance of divalent anion binding to the kinetics and stability of RNase A folding seems clear [3,4]. In the absence of compensating ion uptake or release, anion binding will reduce the valence of RNase A directly. Furthermore, the energetics of any process (e.g., folding, ligand binding, etc.) are affected by any accompanying change in the protein's valence. Consequently, it would be of interest to be able to measure the valence of RNase A to determine whether it is perturbed by ion binding and, if so, to determine how ion binding might contribute to protein folding energetics. Recently, we have shown that accurate protein valence may be determined by free-solution electrophoresis [5,6].

Free-solution electrophoresis can be defined as any electrophoretic method that does not employ a supporting medium, or separate phase, such as a gel. The most widespread free-solution method in current use is capillary electrophoresis (CE),[1] which is a thin-zone method. More recently, a broad-zone, free-solution method, membrane-confined electrophoresis (MCE), has been developed [7]. In principle, both methods should be capable of yielding useful information related to macro-ion charge [6,8]. By virtue of being a thin-zone method, CE is well suited to rapidly test whether a macro-ion sample is heterogeneous with respect to electrophoretic mobility. The spatial and temporal changes in solution composition across macro-ion concentration

* Corresponding author. Fax: +1 603 862 4013.
E-mail address: tpm@cisunix.unh.edu (T.P. Moody).

[1] *Abbreviations used:* CE, capillary electrophoresis; MCE, membrane-confined electrophoresis; BTP, Bis–Tris propane; SSE, steady state electrophoresis; DHH, Debye–Hückel–Henry.

0003-2697/$ - see front matter © 2004 Elsevier Inc. All rights reserved.
doi:10.1016/j.ab.2004.09.009

boundaries in CE, however, complicate the analysis of CE data, as solution composition profoundly affects electrophoretic mobility [9,10]. As a broad-zone method, MCE permits the electrophoretic properties of a macro-ion solution to be studied at thermodynamic steady state [11], eliminating temporal changes in solution composition and producing significantly smaller spatial changes in solution composition than CE does. The disadvantages of MCE are that it can be much more time consuming than CE and it is less well suited than CE to study solutions that contain a heterogeneous mixture of macro-ion components. The thermodynamic steady state capability of MCE, however, should make it better suited than CE to deal with solutions in which mass–action association results in the presence of a single, multispecies, macro-ion component [6].

As an intrinsically absolute approach, free-solution electrophoresis has long held the potential to provide accurate measurements of the charge, Q, of macro-ions in solution. Such measurements would permit the correlation of charge with other macro-ion characteristics, such as solubility, stability, and strength of interactions. The analysis required to determine Q from electrophoretic data, however, is complicated by the fact that the electrophoretic characteristics of a macro-ion in aqueous solution depend not only on the properties of the macro-ion itself but also on the properties of its counter-ions and, to a lesser extent, of its co-ions [12–14].

Counter-ions move opposite to the direction of macro-ions in the presence of an electric field, and the transfer of momentum from the counter-ions to the fluid produces a nonconservative steady state force on the macro-ion that is commonly referred to as the ''electrophoretic effect'' [15,16]. The tendency of the ion atmosphere and the macro-ion to move in opposite directions gives rise to an additional force, referred to as the ''ion relaxation effect'' [16]. Both effects decrease the velocity of the macro-ion from that which would be predicted from simple hydrodynamic and electrostatic considerations. The electrophoretic effect significantly reduces the mobility of any macro-ion, whereas the ion relaxation effect is significant only for more highly charged macro-ions [17].

The magnitudes of the electrophoretic and ion relaxation effects are dependent in a complex manner on the properties of the electrolyte ions and the macro-ions. Furthermore, at low to moderate fields, both effects vary linearly with the electric field, making it impossible to determine their contributions by varying the field strength. Thus, as presently conducted, electrophoretic experiments, by themselves, do not provide sufficient information for the determination of the charge of a macro-ion in solution. However, a substantial body of theoretical work permits estimation of macro-ion valence by the analysis of experimental data.

Within the framework of nonequilibrium thermodynamics, Onsager and Fuoss [18] described the electrophoresis of strong electrolytes phenomenologically, and their approach has been extended to yield a nonequilibrium thermodynamic description of macro-ion solutions in MCE [6,19]. Nonequilibrium thermodynamic analysis of MCE data yields information about the macroscopic electrophoretic properties of macro-ions in solution.

At a detailed, microscopic level, Henry [15] described the electrophoretic mobilities of some classes of spherical and cylindrical particles, unifying the work of Smoluchowski [20] and Debye and Hückel [21] in the process. Overbeek [17] derived the first general formulation of the coupled steady state hydrodynamic, ion transport, and electrodynamic differential equations, which he then applied to the electrophoretic transport of a weakly charged sphere in a weak external electric field. More general treatments have followed in which macro-ions are modeled as charged spheres [16,22,23], long uniformly charged cylinders [24,25], or ''thin double layers'' [26,27].

Allison and co-workers [12–14] generalized the transport theory of Overbeek [17] and Booth [22] to develop a boundary element method that models the electrophoresis of infinitely dilute, rigid macro-ions of arbitrary size, shape, and charge distribution. The modeling incorporates structural and titration data and simultaneously solves the Poisson, Navier–Stokes, and ion transport equations to calculate the electrophoretic mobility of macro-ions. This method has produced results that are in good agreement with the experimentally determined mobilities of hen egg white lysozyme [28], short DNA fragments [29], and charge mutants of T4 lysozyme [5] under a range of conditions. The T4 lysozyme charge mutant studies, in particular, showed that accurate estimates of protein valence can be calculated by the application of the Debye–Hückel–Henry model (see below) to experimentally obtained electrophoretic data.

In this study, valence estimates were obtained by application of the Debye–Hückel–Henry model to the results of the nonequilibrium thermodynamic analysis of MCE experiments with ribonuclease A in buffers of different pH but otherwise identical electrolyte composition. The results reveal that a specific property of the macro-ion, ion binding, can be distinguished and characterized by analytical electrophoresis.

Materials and methods

Protein

Bovine pancreatic RNase A (Beckman Lot No. 5905533) was dissolved to 3.8 mg/mL in 100 mM KCl, 10 mM Bis–Tris propane (BTP), pH 6.50. A single peak

was observed by isoelectric-focusing CE at 500 V/cm using a Beckman Coulter P/ACE 5510 apparatus. Prior to analysis by MCE, samples were dialyzed overnight in the MCE instrument at a low field with the cathode at the top, thus providing convection (RNase A being positively charged) to enhance buffer exchange.

Buffer

All buffers were prepared using reagent-grade chemicals and distilled, deionized water. Buffer pH was determined using an Orion 520A pH meter. Conductivity was measured with a VWR 1054 conductivity meter and platinum electrode. Samples were analyzed in 100 mM KCl, 10 mM BTP buffers at pH 6.00, 6.50, 7.00, 7.50, and 8.00. (The average conductivity was 12.59 mS/cm.) Buffers were changed by dialysis in the MCE instrument.

MCE

The MCE instrument has been described previously [11]. Briefly, macro-ions in solution are confined within a quartz cuvette having square ends that are sealed by semipermeable membranes at the top and bottom. Current flow through the cuvette is carried by ions that are small enough to pass through the membranes. In the work described here, the temperature was held at 20 ± 0.1 °C using a circulating water bath. A 10 mL/h buffer flow through the buffer chambers maintained constant buffer composition outside the cuvette, by virtue of which no significant concentration gradients would be expected to develop in any species, such as BTP, K^+, or Cl^-, that can pass through the membranes [7,11]. Absorbance data at a wavelength of 280 nm were obtained for fixed points within the system using a photodiode array imaging system. The choice of wavelength yielded data proportional to the concentration of membrane-confined species and insensitive to the concentration of membrane-permeant species.

Extensive work has been done with the optically detectable ion, NO_3^-, and pH-sensitive dyes to test for concentration gradients in membrane-permeating species. The development of such gradients can be minimized by a judicious choice of membranes. For the experiments described here, Spectra/Por 8-kDa cut-off membranes, treated with 0.1 mM of 1-ethyl-3-(3-dimethylaminopropyl) carbodiimide HCl and 0.1 mM ethanolamine to minimize the presence of carboxyl groups [30], were used.

The conductivity (κ) of the buffer is measured at the temperature of the experiment and used to estimate the conductivity of the solution in the cuvette, permitting the electric field in the cuvette to be estimated as $i/\kappa A$, where i is the time-invariant current passing through the solution and A is the plane cross-sectional area of the cuvette [6,7,11].

Though the concentrations of small molecules remain fairly uniform throughout the cuvette, it is the development of concentration gradients in membrane-confined species that permits the measurement of the reduced (a.k.a. the effective, apparent, or electrokinetic) valence of such species [6,7]. The reduced valence is obtained from steady state electrophoresis experiments, such as those described below.

Determination of reduced valence, z^*, by steady state electrophoresis

The reduced valence in proton equivalents is determined as

$$z^* = \frac{k_B T w}{eE}, \tag{1}$$

where e ($1.6021892 \times 10^{-19}$ C) is the elementary charge, E (V/cm) is the electric field, k_B (1.38066×10^{-23} J/K) is the mks Boltzmann constant, T (K) is the absolute temperature, and w (cm^{-1}) is the reduced molecular charge of the macro-ion species [6,19]. The reduced valence depends on the properties of the system and is affected by ion flows and, if present, by solvent flow. Thus, z^* is a system parameter. Though z^* is not a molecular parameter, it is the natural parameter obtained from the analysis of SSE data [6].

The reduced valence was determined by SSE using a 2×2-mm square $\times$ 4-mm long cuvette ($A = 0.04$ cm^2) in the MCE instrument [5,7,11,19]. At steady state, the flux due to the electrophoresis of a membrane-confined species is exactly balanced by the flux due to its diffusion at each point in the system. The result is that all system properties, including the concentration gradient of any membrane-confined species, are invariant with time, making SSE analogous to equilibrium sedimentation.

For a system with a single-species macro-ion component, and given certain assumptions [6], the equation describing the macro-ion concentration gradient at steady state is

$$c = a_0^* e^{w(x-x_0)-2MB^*c}, \tag{2}$$

where

$$a_0^* = c_0 e^{2MB^*c_0} \tag{3}$$

is the apparent activity of the macro-ion at x_0, x is the cuvette position in cm, x_0 is the arbitrary reference position; c is the macro-ion concentration at x (the cgs units of mass concentration are g/cm^3, though other units that are proportional to mass concentration, such as the absorbance units obtained experimentally, can be used), c_0 is equal to c at x_0, M is the molar mass, in g/mol, of the macro-ion; B^* is the apparent second virial coefficient that accounts for the apparent influence of c on the exponent of Eq. (2) (the units of B^* are the inverse of the units of Mc), and the previously defined w is the

exponential coefficient that characterizes the steady state concentration gradient in the limit as c approaches zero [6,19].

The apparent influence of c on the exponent of Eq. (2) can include, but is not limited to, the effect that c has on the thermodynamic nonideality of the system. The assumptions underlying Eq. (2) are that any thermodynamic nonideality is proportional to c and that all other apparent influences of c on the exponent are proportional to dc/dx [6].

The establishment of steady state was judged using Match (courtesy of David Yphantis; available at the RASMB archive: ftp://www.bbri.org/rasmb). Absorbance data (at a wavelength of 280 nm) were truncated at the ends of each data set to remove points distorted by reflections from the membranes. Nonlinear least squares analysis was used to determine w [7,31]. For each pH, w was determined for at least five different currents. In all cases, the data fit adequately to a model consisting of a single, nonideal species. Diagnostic graphs of w as a function of E, and w/E as a function of E, were plotted to test for bulk solvent flow [7]. Once it was demonstrated that the steady state distributions were not affected by bulk solvent flow [5], w was determined by nonlinear least squares analysis using the combined data from all currents normalized to the lowest current [7].

Determination of the translational diffusion coefficient, D, by sedimentation

Use of the Debye–Hückel–Henry model (see below) requires knowledge of the Stokes radius of the macroion, which for this work was calculated from the hydrodynamic frictional coefficient, f (in g/s). Determinations of D were made to obtain estimates of f. Values of D (in cm^2/s) were determined directly from modeling of velocity sedimentation boundaries, with D and the sedimentation coefficient, s (in seconds), as fitting parameters of the data analysis program, Sedfit [32]. However, the confidence intervals on these values of D were large. [The larger these confidence intervals are, the greater the uncertainty is in any subsequently calculated Stokes radius and, hence, in any subsequently determined valence (see Debye–Hückel–Henry model).] Consequently, D was calculated from the Svedberg equation,

$$D = \frac{sRT}{M_b}, \tag{4}$$

where R (8.3144×10^7 erg/mol K) is the cgs ideal gas constant and M_b (in g/mol) is the buoyant molar mass. Velocity sedimentation was used to obtain s [32], and equilibrium sedimentation was used to obtain M_b [33]. The values of D calculated in this way were in good agreement with those determined directly from modeling of velocity sedimentation boundaries and have relatively small confidence intervals. However, the values obtained by both of these methods were uniformly higher than those commonly cited (see Appendix).

Velocity sedimentation experiments were conducted in a Beckman Coulter XLA analytical ultracentrifuge at 60,000 rpm, 20 °C, using absorbance detection (at a wavelength of 280 nm) and 12-mm charcoal–epon centerpieces. Data were acquired at 4-min intervals. At pH 7.0, experiments were conducted at RNase A loading concentrations of 0.15, 0.20, and 0.57 mg/mL. (Concentrations at other values of pH are given in Table 1.) The use of multiple concentrations permitted s and D to be extrapolated to s^0 and D^0, their respective values at infinite dilution. As no definitive trend was seen over this concentration range and as all determinations of D, including those at other pH values, were within error of each other, D^0 was taken to be the average of all the values of D in Table 1.

Equilibrium sedimentation experiments were conducted in a Beckman Coulter XLA analytical ultracentrifuge at 20 °C and pH 7.0, with protein loading

Table 1
Sedimentation results

pH[a]	c[a,b] (mg/mL)	s[a,c] ($\times 10^{13}$) (s)	M[a,d] (g/mol)	rms[a,e] A_{280}	D[a,f] ($\times 10^7$) (cm^2/s)
6.0	0.18	1.78 ± 0.05	13,700	0.0043	11.3 ± 0.9
6.5	0.16	1.89 ± 0.05	13,700	0.0054	12.0 ± 0.9
7.0	0.15	2.03 ± 0.03	13,300	0.0046	12.9 ± 0.9
7.0	0.20	1.91 ± 0.03	13,300	0.0046	12.1 ± 0.8
7.0	0.57	1.94 ± 0.03	13,900	0.0056	12.3 ± 0.8
7.5	0.21	1.84 ± 0.05	13,810	0.0046	11.7 ± 0.9

[a] Measurements made in 100 mM KCl, 10 mM BTP at 20 °C.

[b] Determined from A_{280} values returned by Sedfit, using an extinction coefficient at 280 nm of $\varepsilon_{280} = 0.660$ mL/mg cm, and adjusted for the 1.2 cm cell pathlength.

[c] Sedimentation coefficient returned by Sedfit. (Uncorrected to $s_{20,w}$. See Appendix.)

[d] Molecular weight returned by Sedfit, assuming $\bar{v} = 0.72$ mL/g and $\rho = 1.00316$ g/mL, where $\bar{v}$, the partial specific volume, and ρ, the solution density, were both determined using Sednterp.

[e] Root mean square error of the fit of Sedfit to a minimum of 30 scans taken over the course of 2 h.

[f] D calculated using Eq. (4), with $M_b = 3850$ g/mol (3680–4040 g/mol) determined from equilibrium sedimentation. (The value is uncorrected to $D_{20,w}$. See Appendix.) The confidence interval is calculated by combining the worst case errors in s and M_b. No significant concentration dependence was found, so the six values of D were averaged to obtain an estimate of $D^0 = (12.0 \pm 0.9) \times 10^{-7}$ cm^2/s.

concentrations of 0.3, 0.52, 0.9, 1.1, and 2.7 mg/mL in six-channel charcoal–epon centerpieces using absorbance optics (at a wavelength of 280 nm) and rotor speeds of 30,000 and 40,000 rpm. Data were acquired at 1-h intervals and the establishment of equilibrium was determined using Match. Data were edited using WinReedit and analyzed using WinNonlin. (These programs are available at ftp://alpha.bbri.org/rasmb/spin). The analysis of the data permitted the calculation of M_b [33].

Debye–Hückel–Henry model

In the absence of ion relaxation, z^* of a spherical macro-ion containing a centrosymmetric charge distribution is

$$z^* = z\frac{f(\chi\alpha)}{1+\chi\alpha}, \tag{5}$$

where $f(\chi\alpha)$ is Henry's function, χ is the inverse Debye length, α is the radial distance to the surface of shear [5,15,19], and z is the valence ($z = Q/e$). Henry's function accounts for the electrophoretic effect. The sum of the Stokes radii of RNase A and its counter-ion, Cl^-, was used to estimate α. (The Einstein relationship (using the cgs Boltzmann constant) gives $f^0 = k_B\ T/D^0$, and the Stokes equation yields $R_S = f^0/6\pi\eta$, where f^0 is the frictional coefficient of the molecule in question at its infinite dilution, and R_S is the Stokes radius in cm.) Sednterp [34] was used to calculate the solution viscosity, η. Eq. (5) assumes the validity of the linear Poisson–Boltzmann relation in describing the ion distribution around the macro-ion and should be valid for a macro-ion of low zeta potential ($e\zeta/k_B\ T << 1$, where ζ is the zeta potential in V, and k_B is the mks Boltzmann constant).

The equation for the inverse Debye length [35] is

$$\chi = F\sqrt{\frac{2\Gamma}{\varepsilon_0\varepsilon RT}\frac{1000\ \mathrm{L}}{\mathrm{m}^3}\frac{1\ \mathrm{m}}{100\ \mathrm{cm}}}, \tag{6}$$

where F is the Faraday (96,484 C/mol), R is the mks ideal gas constant, ϵ_0 is the permittivity constant (8.85419×10^{-12} C^2/J m), ε is the dielectric constant of the solution, and Γ is the ionic strength.

The equation used for Henry's function was

$$f(\chi\alpha) = 5 - \mathrm{erf}\left(\frac{5}{4}\left[0.10392\{\log(\chi\alpha)\}^2 - 1.10094 \times \log(\chi\alpha) + 0.99302\right]\right)\Big/4, \tag{7}$$

which was obtained by fitting data obtained from Henry's actual function. The values calculated using Eq. (7) are within approximately 0.7% of tabulated values [36] in the region of $\chi\alpha = 2.0$. At approximately $\chi\alpha = 200{,}000$, where $f(\chi\alpha)$ is very nearly 1.5, Eq. (7) reaches a maximum, while the actual Henry's function asymptotically approaches 1.5 as $\chi\alpha$ approaches infinity. (The function given by Eq. (7) reflects about the line $\log(\chi\alpha) \cong 5.3$.) Thus, Eq. (7) cannot be used for $\chi\alpha > 200{,}000$, but for such large values of $\chi\alpha$, the value $f(\chi\alpha) = 1.5$ can just be assumed.

Results and discussion

RNase A was chosen for this work because it is a well-characterized, stable, rigid protein available as an electrophoretically pure molecule. In fact, RNase A is used as a standard in gel electrophoresis, CE, and isoelectric focusing. Furthermore, good structural and ionization data are available for RNase A [37]. These characteristics make RNase A an ideal macro-ion for work that combines experiments and modeling to investigate electrophoretic processes. The electrolyte chosen for this work was KCl. With this choice, the major constituent ions of the solution, K^+ and Cl^-, have transport properties of nearly identical magnitude but opposite direction, thus reducing electroosmotic flows to demonstrably negligible levels [7].

Determination of η, R_S, α, χ, and f(αχ)

For all the solutions in this work, $\eta = 1.0027 \times 10^{-2}$ g/cm s. Also, D^0 of the macro-ion is essentially the same ($12.0 \pm 0.9 \times 10^{-7}$ cm^2/s) in all the solutions (Table 1). Thus, a value of $R_S = 1.78 \times 10^{-7}$ cm (1.66×10^{-7}– 1.93×10^{-7} cm) is obtained for the macro-ion in these solutions. Using $R_S = 1.22 \times 10^{-8}$ cm for Cl^- (based on $D^0 = 175.8 \times 10^{-7}$ cm^2/s [38–40]), the value $\alpha = 1.90 \times 10^{-7}$ cm (1.78×10^{-7}– 2.05×10^{-7} cm) is obtained (see Debye–Hückel–Henry model).

For all the solutions described here, $\varepsilon = 78.5$, $T = 293$ K, and $\Gamma = 0.110$ mol/L, giving $\chi = 1.10 \times 10^7\ cm^{-1}$ by Eq. (6). This value, combined with the value for α, gives $\chi\alpha = 2.10$ (1.96–2.25), and, from Eq. (7), $f(\chi\alpha) = 1.06_3$ (1.05_7–1.06_9). According to Eq. (5), then, the expected slope for a plot of z^* versus z would be 0.344 (0.329–0.358).

pH dependence of z^* for RNase A

The reduced valence of RNase A was determined by SSE (Table 2). For measured values of z^* to be considered accurate it is necessary to (1) demonstrate that the concentration profile fits well to a to model consisting of a single species, (2) show that w increases linearly with E, and (3) test for contributions to w from bulk solvent flow [7]. The concentration profiles for RNase A fit well to a model consisting of a single nonideal species. A linear fit of w as a function of E showed that w does increase linearly with E. The fit also yields a y intercept that, within error, encompasses zero, indicating that

Table 2
Steady state electrophoresis results

pH	$2MB^{*}$[a] (low, high) (mol/g A_{280})	z^{*}[b,c] (low,high)	z[d] (low, high)	z_f[e]		z/z_f	
				apo	holo	apo (low, high)	holo (low, high)
6.0	1.179 (0.600, 1.783)	1.180 (1.074, 1.290)	3.430 (3.000, 3.921)	5.95	3.95	0.577 (0.504, 0.659)	0.868 (0.759, 0.993)
6.5	0.046 (−0.051, 0.146)	0.940 (0.887, 0.994)	2.762 (2.478, 3.021)	5.00	3.00	0.552 (0.496, 0.604)	0.921 (0.826, 1.007)
7.0	6.5×10^{-4} (−0.081, 0.084)	0.760 (0.731, 0.790)	2.209 (2.042, 2.401)	4.40	2.40	0.502 (0.464, 0.546)	0.921 (0.851, 1.001)
7.5	0.803 (0.449, 1.165)	0.700 (0.658, 0.743)	2.020 (1.899, 2.144)	4.11	2.11	0.491 (0.462, 0.522)	0.957 (0.900, 1.016)
8.0	0.383 (0.241, 0.528)	0.600 (0.574, 0.627)	1.744 (1.560, 1.906)	3.94	1.94	0.443 (0.407, 0.484)	0.899 (0.826, 0.982)

[a] The parameter $2MB^{*}$ of Eq. (2) was included in the data fitting. The units result from using A_{280} data for c in Eq. (1).
[b] Measurements made in 100 mM KCl, 10 mM BTP at 20 °C. Fits yielded w, which was converted to z^{*} using Eq. (1). An overall RNase A concentration in the cuvettes of 2.78 mg/mL was determined from A_{280} values measured experimentally, using an extinction coefficient at 280 nm of $\varepsilon_{280} = 0.660$ mL/mg cm, and adjusted for the 0.2 cm cell pathlength.
[c] Reduced valence determined from SSE measurements using Eq. (1). Uncertainty is estimated for the 95% confidence level.
[d] Valence calculated from z^{*} using Eq. (5), with α determined using the average $D^{0} = (12.0 \pm 0.9)\times 10^{-7}$ cm^2/s for RNase A and $D^{0} = 175.8\times 10^{-7}$ cm^2/s for Cl^{-} [38–40].
[e] Formal valence calculated from pK_a data as described under Materials and methods for RNase A lacking (apo) and containing (holo) two bound monovalent anions.

there is no significant field-independent bulk fluid flow [7]. A more sensitive test for both the linearity of w with E and the bulk fluid flow is obtained from a graph of the ratio of w/E versus E. No systematic deviation of w/E with E is seen in these graphs, which indicates a lack of valence heterogeneity and shows that the data are unaffected by bulk solvent (i.e., nonelectroosmotic) flow dependent on E^{n}, for $n \neq 1$ [7]. Monitoring the concentration profile of an uncharged macromolecule in the presence of an electric field provides an independent test for bulk solvent flow. Using rhodamine dextran, it has been shown that 10 mM Tris, pH 8.0, 100 mM KCl produces negligible bulk solvent flows for fields as high as 6 V/cm [7]. The substitution of 10 mM BTP for 10 mM Tris, checked at pH 6.0 and 7.5, has a negligible impact on bulk solvent flow.

The values of z^{*} at each pH are presented in Table 2 along with the formal valence, z_f (apo-RNase A), calculated from the measured pK_a data [37]. As is expected from theory, z^{*} is substantially less than z_f [26,41]. Both z^{*} and z_f decrease with increasing pH. The ratio of z^{*}/z_f, however, is not constant with pH, indicating that there are changes in the electrohydrodynamic characteristics of RNase A in these buffers over this pH range or that the valence of the protein is changing by mechanisms that are not modeled in the calculation of z_f, such as the binding of chloride. (RNase A with two chlorides bound is referred to as holo-RNase A in this paper.) These two possibilities are not mutually exclusive, as changes in the macromolecular valence can cause changes in the electrohydrodynamic characteristics.

Though it is not possible to determine macromolecular valence independently of the electrohydrodynamic characteristics by currently available experimental means alone, information about their relative contributions to z^{*} can be obtained from a comparison of experimental results with the results from modeling, either by boundary element methods or by application of the DHH equation (Eq. (5)), as shown in the previous T4 lysozyme study [5]. (Boundary element modeling of lysozyme [5,28] showed that the valence of typical globular proteins can be determined from experimental data using the DHH model.) Application of the DHH model to the experimental data produced the experimentally determined estimates of z presented in Table 2.

Along with z_f of apo RNase A, z_f of holo RNase A, in which two additional negative charges are assumed to be bound to the macro-ion, was calculated (Table 2). The results in Table 2 show that z best matches z_f of holo RNase A, for which z/z_f is constant with pH, within the error of that value. On this basis, the data and

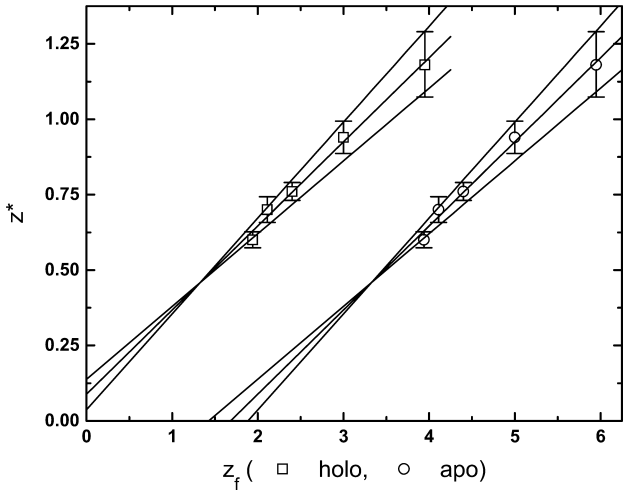

Fig. 1. Comparison of reduced valence with calculated valence. Experimental values of z^{*} versus z_f for RNase A with (holo, □, minimum values of $z^{*} = (0.24129 \pm 0.01683)\times z_f + 0.13815 \pm 0.04675$, central values of $z^{*} = (0.2789 \pm 0.01471) \times z_f + 0.08855 \pm 0.01471$, maximum values of $z^{*} = (0.31794 \pm 0.0161)\times z_f + 0.03672 \pm 0.04472$) and without (apo, ○, minimum values of $z^{*} = (0.24129 \pm 0.01683)\times z_f - 0.34442 \pm 0.07972$, central values of $z^{*} = (0.2789 \pm 0.01471)\times z_f - 0.46925 \pm 0.06968$, maximum values of $z^{*} = (0.31794 \pm 0.0161)\times z_f - 0.59916 \pm 0.07625$) two anions bound.

Table 3
Electrostatic free energy change with binding of two chlorides

pH	z_f[a]		ΔG_{EL}[b] (low[c] D^0, high[d] D^0) (kJ/mol)	z[e] (low, high)	ΔG_{EL}[f] (low[c] D^0 and high z, high[d] D^0 and low z) (kJ/mol)
	apo	holo			
6.0	5.95	3.95	−3.606 (−3.173, −4.055)	3.430 (3.000, 3.921)	−4.305 (−3.210, −5.993)
6.5	5.00	3.00	−2.914 (−2.564, −3.277)	2.762 (2.478, 3.021)	−3.164 (−2.544, −3.862)
7.0	4.40	2.40	−2.477 (−2.180, −2.785)	2.209 (2.042, 2.401)	−2.637 (−2.179, −3.111)
7.5	4.11	2.11	−2.266 (−1.994, −2.548)	2.006 (1.807, 2.231)	−2.343 (−1.910, −2.791)
8.0	3.94	1.94	−2.142 (−1.885, −2.408)	1.744 (1.560, 1.906)	−2.273 (−1.906, −2.681)

[a] Formal valence calculated from pK_a data as described under Materials and methods for RNase A lacking (apo) and containing (holo) two bound monovalent anions.

[b] ΔG_{EL} calculated using Eq. (8), with α and β determined using $D^0 = 12.0 \times 10^{-7}$ cm^2/s for RNase A and $D^0 = 175.8 \times 10^{-7}$ cm^2/s for Cl$^-$.

[c] ΔG_{EL} calculated using Eq. (8), with α and β determined using $D^0 = (12.0–0.9) \times 10^{-7}$ cm^2/s for RNase A and $D^0 = 175.8 \times 10^{-7}$ cm^2/s for Cl$^-$.

[d] $\Delta G_{EL} = G_{ELholo} - G_{ELapo}$, where G_{ELholo} is G_{EL} of the holo enzyme and G_{ELapo} is G_{EL} of the apo enzyme (see Eq. (8)), with α and β determined using $D^0 = (12.0 + 0.9) \times 10^{-7}$ cm^2/s for RNase A and $D^0 = 175.8 \times 10^{-7}$ cm^2/s for Cl$^-$.

[e] Valence calculated from z^* using Eq. (5), with α determined using the average $D^0 = (12.0 \pm 0.9) \times 10^{-7}$ cm^2/s for RNase A and $D^0 = 175.8 \times 10^{-7}$ cm^2/s for Cl$^-$ [38–40].

[f] $\Delta G_{EL} = G_{ELexp} - G_{ELapo}$, where G_{ELexp} is G_{EL} calculated with the experimentally determined z (and its range) and G_{ELapo} is G_{EL} of the apo enzyme (see Eq. (8)), with α and β determined using $D^0 = (12.0 + 0.9) \times 10^{-7}$ cm^2/s for RNase A and $D^0 = 175.8 \times 10^{-7}$ cm^2/s for Cl$^-$.

analysis can be taken as evidence of previously suggested anion binding by RNase A [1]. Fig. 1 shows that a plot of the highest range values of z^* versus the holo or apo RNase A z_f values comes closest to the expected slope of 0.344 (0.329–0.358) and that a plot of the highest range values of z^* versus the holo RNase A z_f values best conforms to the expectation that the line should intercept the origin. The x intercept of the z^* versus apo RNase A z_f values is 1.683 (1.025–2.238), which provides an estimate of the anion equivalents bound. Anion binding by RNase A is plausible. Most crystal structures of RNase A (3RN3, for example [42]) indicate that an anion, such as SO_4^{2-}, may be coordinated between His-12 and His-119. Anion binding would reduce the valence, and thus z^*, of the macro-ion.

The electrostatic free energy of the macro-ion in solution is approximately

$$G_{EL} = \frac{(ze)^2 N_A}{8\pi\varepsilon_0\varepsilon\beta}\left(\frac{1+\chi[\alpha-\beta]}{1+\chi\alpha}\right)\frac{100\text{ cm}}{\text{m}}, \quad (8)$$

where β is the Stokes radius of the macro-ion and N_A is Avogadro's number [35]. Table 3 shows $\Delta G_{EL} = G_{ELholo} - G_{ELapo}$ (where G_{ELholo} is G_{EL} of the holo enzyme and G_{ELapo} is G_{EL} of the apo enzyme), along with $\Delta G_{EL} = G_{ELexp} - G_{ELapo}$ (where G_{ELexp} is G_{EL} calculated with the experimentally determined z). The results show that the binding of two chlorides is thermodynamically favorable, as it reduces the self-potential of the enzyme by approximately 2 kJ/mol at pH 6.0 and by 4 kJ/mol at pH 8.0.

It should be noted that RNase A is expected to be asymmetric [42] and that to calculate z using Eq. (5) the protein is described with regard to its equivalent sphere, the radius of which is treated as the Stokes radius of the protein. Furthermore, as z^* of an asymmetric particle is expected to be less than z^* of a spherical particle with the same valence and volume [43], it could be argued that the values of z listed for holo RNase A in Table 2 are minimum values. However, the Stokes radius of an asymmetric particle is expected to be greater than the radius of a spherical particle of equal volume [44]. Thus, any underestimate of z resulting from the use of the Stokes radius to calculate α in Eq. (5) will be less than the underestimate that would result if the radius of an equal-volume sphere were used instead. The extent to which use of the Stokes radius minimizes underestimates of z for asymmetric particles is not known, but previous results [5] suggest that the magnitude of the error is likely to fall within the uncertainty in z.

Acknowledgments

This research was supported in part by National Science Foundation Grants MCB-9807541, BIR 9314040, and MCB 9807550.

Appendix

It was the unpublished work of C.F. Vilbrandt, H.G. Tennent, and N.V. Hakala, mentioned in passing in a paper by Bridgman and Williams [45] and later cited by Overbeek [46], that is the source of the oft cited 10.2 F (1 F = 10^{-7} cm^2/s) value for the D_{20} (D at 20 °C) of ribonuclease. The source of this ribonuclease was not mentioned, nor the solution conditions, other than mention that the work was conducted at around 20 °C. Bridgman and Williams do say that the protein "had stood in the dry condition for some weeks and it is quite possible it had undergone some denaturation on standing," so that "some modification in the values of s and D is to be expected." Thus, a more extensive

search of the literature was undertaken, and new experiments conducted, to obtain reliable estimates of D^0 and $D^0_{20,w}$ (D^0 in water at 20 °C) for bovine ribonuclease A.

Materials and methods

Sednterp [47] was used to obtain the values of ρ needed for standardizing s and the values of η needed for standardizing both s and D to water at 20 °C. The values of $\bar{v}$ needed to standardize s to water at 20 °C were obtained from sedimentation data and prior knowledge of M, using

$$\bar{v} = \frac{M - M_b}{M\rho}, \tag{A.1}$$

obtained by solving the equation $M_b = M(1 - \bar{v}\rho)$ for $\bar{v}$.

Analysis of the equilibrium sedimentation data obtained with RNase A in 100 mM KCl, 10 mM BTP at pH 7.0 and 20 °C yielded $M_b = 3850$ (3680–4040). From this estimate of M_b, an estimate of $\bar{v} = 0.72 \pm 0.01$ mL/g is obtained using the sequence molar mass, M_s, of 13,816 g/mol, for M in Eq. (A.1). This approach to estimating $\bar{v}$ has the virtue of combining the experimentally determined results with the best previous knowledge, in the form of M_s, available. This value obtained is higher than that calculated from the composition, 0.7097 mL/g, using Sednterp. (It is also higher than the value of 0.710 mL/g obtained by Rothen [48] using density measurements of solutions of known concentrations of RNase A in either pure water or 500 mM $(NH_4)SO_4$ at 25 °C.)

It was assumed that the partial specific volume has the same value, 0.72 mL/g, for RNase in the solution at the experimental temperature (20 °C) and water at 20 °C, denoted as $\bar{v}$ and $\bar{v}_{20,w}$, respectively. For the solutions at 20 °C, $\rho = 1.00316$ g/mL and $\eta = 1.0027 \times 10^{-2}$ g/cm s, while for water at 20 °C, $\rho_{20,w} = 0.99823$ g/mL and $\eta_{20,w} = 1.009 \times 10^{-2}$ g/cm s. The standardized values of s and D are denoted as $s_{20,w}$ and $D_{20,w}$, respectively, and $s_{20,w}$ and $D_{20,w}$ at infinite dilution are denoted as $s^0_{20,w}$ and $D^0_{20,w}$, respectively. (These standardized values are presented only for purposes of comparison with other results. They are not used in the calculation of z from z^*, which requires D^0.) The correction equations are

$$s_{20,w} = \frac{(1 - \bar{v}_{20,w}\rho_{20,w})\eta}{(1 - \bar{v}\rho)\eta_{20,w}}, \tag{A.2}$$

and

$$D_{20,w} = \frac{293.15\ \text{K}}{T}\frac{\eta}{\eta_{20,w}}D \tag{A.3}$$

[49]. The application of these equations to values of s or D obtained in solvents other than pure water or temperatures other than 293.15 K are not expected to yield accurate estimates of $s_{20,w}$ or $D_{20,w}$ [49], but the practice of making such conversions is long standing.

Results

See Determination of the translational diffusion coefficient, D, by sedimentation and Eq. (4) of the text for the method used to obtain D^0. Eq. (A.3) was used to obtain $D^0_{20,w}$ from D^0. The resulting estimate of $D^0_{20,w}$, 12.2 ± 0.9 F, is significantly higher than the oft-tabulated values in the literature citing the work of van Holde and Baldwin [50] or Creeth [51]. A close reading of this literature reveals, however, that the estimates of $D_{20,w}$ therein were obtained at protein concentrations of 2.7–10.5 mg/mL and were not extrapolated to zero protein concentration. Furthermore, where concentration dependence data are available, a significant decrease in $D_{20,w}$ is seen with increasing concentration [50]. It should be noted that van Holde and Baldwin used an approach to sedimentation equilibrium method to determine D, and their experiments were conducted "near" 25 °C, at which temperature, the pH of the 150 mM KCl, 7 mM monobasic/dibasic potassium phosphate buffer used was 7.7 [50]. The viscosity of this buffer, calculated using Sednterp, is 0.8900×10^{-2} g/cm s. Their diffusion coefficients were calculated assuming $\bar{v} = 0.728$ mL/g, which had been reported previously by Buzzel and Tanford [52], and corrected to water at 25 °C. Extrapolating the data of van Holde and Baldwin to zero protein concentration and applying Eq. (A.3) yields $D^0_{20,w} = 12.4$ F.

Creeth [51] measured the diffusion coefficient of RNase A using a diffusiometer with a Rayleigh optical system, but the sample was heterogeneous, which would have contributed to an underestimate of D if the contaminating materials that were suspected to be present had lower diffusion coefficients than RNase A. The experiments were conducted at 25 °C, at which temperature, the pH of the 100 mM KCl, 35 mM monobasic/dibasic potassium phosphate buffer used was 7.74. The viscosity of this buffer, calculated using Sednterp, is 0.8993 $\times 10^{-2}$ g/cm s. Creeth did not have data permitting extrapolation to zero concentration but did correct his measurement to 20 °C and water to obtain $D_{20,w} = 10.68$ F.

Rothen [48], whose work is also sometimes found cited in the literature, used a Tiselius apparatus equipped with Schlieren optics to obtain $D = 13.6$ F for RNase A at a concentration of 1% at 25 °C in 500 mM $(NH_4)SO_4$, with the pH unspecified. Using $\eta = 1.0027 \times 10^{-2}$ g/cm s (the solvent viscosity computed using Sednterp) in Eq. (A.3) yields $D_{20,w} = 11.9$ F. No extrapolation to zero concentration is possible from the data.

In the work conducted for this paper, $D_{20,w}$ was determined from combined equilibrium and velocity sedimentation data (obviating any need to know $\bar{v}$) at

each pH used in electrophoresis experiments, including three protein concentrations at pH 7.0 to permit extrapolation to $c = 0$ (see Table below). Under the conditions of these experiments, there was no apparent dependence of $D_{20,w}$ on concentration or pH (see Table below), so the average, 12.2 ± 0.9 F, is assumed to be equal to $D^0_{20,w}$. This value compares favorably with that obtained from the data of van Holde and Baldwin. It also compares favorably with the value reported by Rothen, but given the solution conditions used by Rothen, that value is of limited use for comparison with the work conducted for this paper. It is significantly higher than the value reported by Creeth, but as noted, the heterogeneity of the sample involved could explain the relatively low value that he determined.

Correction of sedimentation results to water at 20 °C

pH[a]	c[a,b] (mg/mL)	$s_{20,w}$[a,c] ($\times 10^{13}$) (s)	$D_{20,w}$[a,d] ($\times 10^{7}$) (cm^2/s)
6.0	0.18	1.80 ± 0.05	11.4 ± 0.9
6.5	0.16	1.91 ± 0.05	12.1 ± 0.9
7.0	0.15	2.06 ± 0.03	13.0 ± 0.9
7.0	0.20	1.93 ± 0.03	12.2 ± 0.8
7.0	0.57	1.97 ± 0.03	12.5 ± 0.8
7.5	0.21	1.86 ± 0.05	11.8 ± 0.9

[a] Measurements made in 100 mM KCl, 10 mM BTP at 20 °C.

[b] Determined from A_{280} values returned by Sedfit, using an extinction coefficient at 280 nm of $\varepsilon_{280} = 0.660$ mL/mg cm and adjusted for the 1.2-cm cell pathlength.

[c] Sedimentation coefficient returned by Sedfit (see Table 1), corrected to $s_{20,w}$.

[d] D calculated from $s_{20,w}$ using the Svedberg equation and using $M_b = 3850$ g/mol (3680–4040 g/mol) determined from equilibrium sedimentation. The confidence interval is calculated by combining worst case errors in $s_{20,w}$ and M_b.

References

[1] J.B. Matthews, F.M. Richards, Anion binding and pH-dependent electrostatic effects in ribonuclease, Biochemistry 21 (1982) 4989–4999.

[2] S. Baubet-Nessler, M. Jullien, M.-P. Crosio, J. Janin, Crystal structure of a fluorescent derivative of RNase A, Biochemistry 32 (1993) 8457–8464.

[3] L.K. Low, H.-C. Shin, M. Narayan, W.J. Wedemeyer, H.A. Scheraga, Acceleration of oxidative folding of bovine pancreatic ribonuclease A by anion-induced stabilization and formation of structured native-like intermediates, FEBS Lett. 472 (2000) 67–72.

[4] C.H.I. Ramos, R.L. Baldwin, Sulfate anion stabilization of native ribonuclease A both by anion binding and by the Hofmeister effect, Protein Sci. 11 (2002) 1771–1778.

[5] J.A. Durant, C. Chen, T.M. Laue, T.P. Moody, S.A. Allison, Use of T4 lysozyme charge mutants to examine electrophoretic models, Biophys. Chem. 101–102 (2002) 593–609.

[6] T.P. Moody, H.K. Shepard, Nonequilibrium thermodynamics of membrane-confined electrophoresis, Biophys. Chem. 108 (2004) 51–76.

[7] T.M. Laue, H.K. Shepard, T.M. Ridgeway, T.P. Moody, T.J. Wilson, Membrane-confined analytical electrophoresis, in: G.K. Ackers, M.L. Johnson (Eds.), Methods in Enzymology, Academic Press, New York, 1998, pp. 479–490.

[8] D.J. Winzor, Determination of the net charge (valence) of a protein: a fundamental but elusive parameter, Anal. Biochem. 325 (2004) 1–20.

[9] P. Gebauer, P. Boček, Predicting peak symmetry in capillary zone electrophoresis: the concept of the peak shape diagram, Anal. Chem. 69 (1997) 1557–1563.

[10] S. Hjertén, Zone broadening in electrophoresis with special reference to high-performance electrophoresis in capillaries: an interplay between theory and practice, Electrophoresis 11 (1990) 665–690.

[11] T.M. Ridgeway, D.B. Hayes, T.P. Moody, T.J. Wilson, A.L. Anderson, J.H. Levasseur, P.D. Demaine, B.E. Kenty, T.M. Laue, An apparatus for membrane-confined analytical electrophoresis, Electrophoresis 19 (1998) 1611–1619.

[12] S.A. Allison, V.T. Tran, Modeling the electrophoresis of rigid polyions: application to lysozyme, Biophys. J. 68 (1995) 2261–2270.

[13] S.A. Allison, Modeling the electrophoresis of rigid polyions: inclusion of ion relaxation, Macromolecules 29 (1996) 7391–7401.

[14] S.A. Allison, H. Wang, T.M. Laue, T.J. Wilson, J.O. Wooll, Visualizing ion relaxation in the transport of short DNA fragments, Biophys. J. 76 (1999) 2488–2501.

[15] D.C. Henry, The cataphoresis of suspended particles. Part I.—The equation of cataphoresis, Proc. R. Soc. A. 133 (1931) 106–140.

[16] P.H. Wiersema, A.L. Loeb, J.T.G. Overbeek, Calculation of the electrophoretic mobility of a spherical colloid particle, J. Colloid Interface Sci. 22 (1966) 78–99.

[17] J.T.G. Overbeek, Theorie der electrophorese. Der Relaxationseffekt, Kolloid-Beih. 54 (1943) 287–364.

[18] L. Onsager, R. Fuoss, Irreversible processes in electrolytes. Diffusion, conductance, and viscous flow in arbitrary mixtures of strong electrolytes, J. Phys. Chem. 36 (1932) 2689–2778.

[19] J.E. Godfrey, Steady-state electrophoresis: a technique for measuring physical properties of macro-ions, Proc. Natl. Acad. Sci. USA 86 (1989) 4479–4483.

[20] M. von Smoluchowski, Versuch einer mathematischen Theorie der Koagulationskinetik kolloider lösungen, Z. Phys. Chem. 92 (1917) 129–168.

[21] P. Debye, E. Hückel, Zur theorie der elektrolyte II. Das Grenzgesetz für die elektrische leifähigkeit, Physik. Z. 24 (1923) 305–325.

[22] F. Booth, The catephoresis of spherical, solid non-conducting particles in a symmetrical electrolyte, Proc. R. Soc. A. 203 (1950) 514–533.

[23] R.W. O'Brien, L.R. White, Electrophoretic mobility of a spherical colloidal particle, Trans. Faraday Soc. 74 (1978) 1607–1626.

[24] D. Stigter, Electrophoresis of highly charged colloidal cylinders in univalent salt solutions. 1. Mobility in transverse field, J. Phys. Chem. 82 (1978) 1417–1423.

[25] D. Stigter, Electrophoresis of highly charged colloidal cylinders in univalent salt solutions. 2. Random orientation in external field and application to polyelectrolytes, J. Phys. Chem. 82 (1978) 1424–1429.

[26] R.W. O'Brien, The solution of the electrokinetic equations for colloidal particles with thin double layers, J. Colloid Interface Sci. 92 (1983) 204–216.

[27] Y.E. Solomentsev, Y. Pawar, J.L. Anderson, Electrophoretic mobility of nonuniformly charged spherical particles with polarization of the double layer, J. Colloid Interface Sci. 158 (1993) 1–9.

[28] S.A. Allison, M. Potter, J.A. McCammon, Modeling the electrophoresis of lysozyme. II. Inclusion of ion relaxation, Biophys. J. 73 (1997) 133–140.

[29] S.A. Allison, S. Mazur, Modeling the free solution electrophoretic mobility of short DNA fragments, Biopolymers 46 (1998) 359–373.
[30] R. Timkovich, Determination of the stable addition of carbodimide to proteins, Anal. Biochemistry 79 (1977) 135–143.
[31] M.L. Johnson, J.J. Correia, D.A. Yphantis, H.R. Halvorson, Analysis of data from the analytical ultracentrifuge by nonlinear least-squares techniques, Biophys. J. 36 (1981) 575–588.
[32] P. Schuck, Sedimentation analysis of noninteracting and self-associating solutes using numerical solutions to the Lamm equation, Biophys. J. 75 (1998) 1503–1512.
[33] T.M. Laue, Sedimentation equilibrium as a thermodynamic tool, Methods Enzymol. 259 (1995) 427–452.
[34] T.M. Laue, B.D. Shah, T.M. Ridgeway, S.L. Pelletier, Computer-aided interpretation of analytical sedimentation data for proteins, in: S.E. Harding, A.J. Rowe, J.C. Horton (Eds.), Analytical Ultracentrifugation in Biochemistry and Polymer Science, Royal Society of Chemistry, Cambridge, UK, 1992, pp. 90–125.
[35] C. Tanford, Electrostatic free energy and polyelectrolytes, in: Physical Biochemistry of Macromolecules, John Wiley and Sons, New York, 1961, pp. 457–524.
[36] J.R. Cann, Principles of electrophoresis and ultracentrifugation, in: Interacting Macromolecules: The Theory and Practice of Their Electrophoresis, Ultracentrifugation, and Chromatography, Academic Press, New York, 1970, pp. 1–46.
[37] J. Antosiewicz, J.M. Briggs, A.H. Elcock, M.K. Gilson, J.A. McCammon, Computing the ionization states of proteins with a detailed charge model, J. Comput. Chem. 17 (1996) 1633–1644.
[38] H.B. Bull, Ion transport, in: An Introduction to Physical Biochemistry, F.A. Davis Company, Philadelphia PA, 1964, pp. 270–293.
[39] R.C. Weast, Editor. Diffusion coefficients of strong electrolytes. in: CRC Handbook of Chemistry and Physics, 58th ed., CRC Press, Cleveland, OH, 1977–1978, p. F-62.
[40] G.W. Castellan, Electrical conduction, in: Physical Chemistry, third ed., Addison-Wesley Publishing, Reading, MA, 1983, pp. 765–797.
[41] J.A. Schellman, D. Stigter, Electrical double layer, zeta potential, and electrophoretic charge of double-stranded DNA, Biopolymers 16 (1977) 1415–1434.
[42] B. Howlin, D.S. Moss, G.W. Harris, Segmented anisotropic refinement of bovine ribonuclease A by the application of the rigid-body TLS model, Acta Cryst. A45 (1989) 851–861.
[43] H.A. Abramson, M.H. Gorin, L.S. Moyer, The polar groups of protein and amino acid surfaces in liquids, Chem. Rev. 24 (1939) 345–366.
[44] K.E. van Holde, W.C. Johnson, P.S. Ho, Methods for the separation and characterization of macromolecules, in: Principles of Physical Biochemistry, Prentice-Hall, Upper Saddle River, NJ, 1998, pp. 192–241.
[45] W.B. Bridgman, J.W. Williams, Optical problems of the ultracentrifuge, Ann. N. Y. Acad. Sci. 43 (1942) 195–210.
[46] J.T.G. Overbeek, Theorie der electrophorese. Der Relaxationseffekt, Kolloid-Beih. 54 (1943) 287–364.
[47] T.M. Laue, B.D. Shah, T.M. Ridgeway, S.L. Pelletier, Computer-aided interpretation of analytical sedimentation data for proteins, in: S.E. Harding, A.J. Rowe, J.C. Horton (Eds.), Analytical Ultracentrifugation in Biochemistry and Polymer Science, Royal Society of Chemistry, Cambridge, UK, 1992, pp. 90–125.
[48] A. Rothen, Molecular weight and electrophoresis of crystalline ribonuclease, J. Gen. Physiol. 24 (1940) 203–211.
[49] C. Tanford, Transport processes, in: Physical Biochemistry of Macromolecules, John Wiley and Sons, New York, 1961, pp. 317–456.
[50] K.E. van Holde, R.L. Baldwin, Rapid attainment of sedimentation equilibrium, J. Am. Chem. Soc. 62 (1958) 734–743.
[51] J.M. Creeth, Studies of free diffusion in liquids with the Rayleigh method. III. The analysis of known mixtures and some preliminary investigations with proteins, J. Phys. Chem. 62 (1958) 66–74.
[52] J.G. Buzzel, C. Tanford, The effect of charge and ionic strength on the viscosity of ribonuclease, J. Phys. Chem. 60 (1956) 1204–1207.